Watching dark solitons decay into vortex rings in a Bose-Einstein condensate

B. P. Anderson,[1,2] P. C. Haljan,[1] C. A. Regal,[3] D. L. Feder,[4] L. A. Collins,[5] C. W. Clark,[4] and E. A. Cornell[1,2]
[1] *JILA, National Institute of Standards and Technology and Department of Physics, University of Colorado, Boulder, Colorado 80309-0440*
[2] *Quantum Physics Division, National Institute of Standards and Technology, Boulder, CO 80305*
[3] *Physics Department, Lawrence University, P.O. Box 599, Appleton, WI 54912*
[4] *Electron and Optical Physics Division, National Institute of Standards and Technology, Gaithersburg, MD 20899-8410*
[5] *Theoretical Division, Mail Stop B212, Los Alamos National Laboratory, Los Alamos, NM 87545*
(February 1, 2008)

We have created spatial dark solitons in two-component Bose-Einstein condensates in which the soliton exists in one of the condensate components and the soliton nodal plane is filled with the second component. The filled solitons are stable for hundreds of milliseconds. The filling can be selectively removed, making the soliton more susceptible to dynamical instabilities. For a condensate in a spherically symmetric potential, these instabilities cause the dark soliton to decay into stable vortex rings. We have imaged the resulting vortex rings.

Topological structures such as vortices and vortex rings have fascinated scientists and mathematicians for centuries. In a quantum fluid, vortices have quantized flow around a one-dimensional core where the density vanishes. Vortex *lines*, which terminate at the boundaries of the quantum fluid, have been observed in superfluid helium and superconductors [1,2], and recently in Bose-Einstein condensates (BECs) [3,4]. Similarly, vortex *rings* are vortices whose cores are closed loops; the poloidal quantized flow pattern resembles that of a smoke ring. Quantized vortex rings have been produced in superfluid helium, and were first detected in pioneering work by Rayfield and Reif [5]. In this paper, we report the first direct experimental observations of vortex rings in BECs.

Solitons are localized disturbances in a continuous nonlinear medium that preserve their spatial profile due to a balance between the effects of dispersion and nonlinearity [6]. Dark solitons have been previously created in single-component BECs using phase-imprinting methods [7]. These structures are characterized by a local decrease in fluid density (the depth). The macroscopic quantum phase of the BEC differs on either side of the soliton; for a completely dark (black) soliton, the depth is 100% (a complete absence of fluid), the phase offset is π, and the soliton velocity is zero. We have created black solitons (having a fluid-free nodal plane) in nearly spherically symmetric ^{87}Rb BECs, and have observed the subsequent decay of the solitons into vortex rings.

Unlike vortices and vortex rings, whose stability is ensured by Kelvin's theorem [1], soliton stability depends on the nonlinearity and geometry of the medium [8]. Optical dark solitons in self-defocusing nonlinear media have been observed to decay into optical vortices via a 'snake instability' [9], confirming predictions [10]. In general, dark solitons in BECs are also expected to be inherently dynamically unstable [11–14]. Because both the velocity and depth of a soliton are determined by its phase offset [15], small local perturbations of either the strength of the nonlinearity or of the depth give the soliton a corresponding nonuniform transverse velocity profile. Once the soliton begins to decay, it quickly breaks up into more stable structures. Within our spherically symmetric BECs, the expected decay products are concentric vortex rings [14]. Because the theoretical background for soliton decay in condensates has been previously described in detail in Ref. [14], we limit our paper to primarily a phenomenological presentation of data. Evidence for soliton decay is obtained through direct images of the BEC density distribution. We provide a visual comparison of data with numerical simulations of soliton decay.

Experimental techniques – We create dark solitons using concepts that we have previously applied to making singly quantized vortices in BECs [3,16]. The magnetically trapped BEC can exist as a superposition of two internal components, hyperfine states $|1\rangle \equiv |F=1, m_F=-1\rangle$ and $|2\rangle \equiv |F=2, m_F=1\rangle$. Conversion between the two components is achieved with a microwave field slightly detuned from the $|1\rangle$ to $|2\rangle$ internal conversion energy. A "modulation beam," an off-resonant laser beam whose small spatial focus provides a requisite spatial selectivity, is dithered rapidly across the BEC. The laser beam induces a small ac Stark shift in the $|1\rangle$ to $|2\rangle$ transition energy. The phase and amplitude of this effective fm modulation varies from point-to-point in the sample in a spatial pattern determined by the time-varying position of the optical modulation beam; thus the microwave-induced inter-component conversion varies in phase and amplitude across the BEC.

In our experiment, we start with a uniform-phase (i.e., ground state) condensate of component $|2\rangle$. To make a soliton, we choose a modulation beam pattern such that inter-component conversion is suppressed in the middle of the sample, whereas the upper and lower parts of the BEC undergo conversion to component $|1\rangle$ with an initial phase offset of π between the two parts. Uncon-

trolled variations in the timing of the modulation cause the angular orientation of the soliton nodal plane to vary randomly from one soliton to the next. For further details, see our earlier vortex work [3] and theory by Williams and Holland [16]. The soliton state contains about 3×10^5 $|1\rangle$ atoms, and the filling consists of about 7×10^5 $|2\rangle$ atoms. The axial (vertical) trap frequency is 7.6(3) Hz, the radial (horizontal) frequencies are 7.8(3) Hz, and the condensates have a Thomas-Fermi (TF) radius of 28 μm. The solitons are created at temperatures of $T = 23(6)$ nK, or $T/T_c = 0.8(1)$, where T_c is the BEC phase transition temperature.

After removing the coupling field, we observe the trapped excited-state condensates using nondestructive phase-contrast imaging. Our probe laser is tuned such that only component $|1\rangle$ is visible, and these atoms appear bright on a dark background. As described in [3], a filled-core vortex appears as a dark hole in a bright atom cloud. Similarly, a soliton with a filled nodal plane appears as a dark band that divides the $|1\rangle$ BEC. This two-component BEC can be described as a *bright* soliton of component $|2\rangle$ trapped within the $|1\rangle$ dark soliton [17]. The filling material of $|2\rangle$ atoms stabilizes the dark soliton against dynamical instabilities; the filled solitons are observed to last for at least 800 ms.

To study the dynamical instabilities of the solitons, we first use resonant light pressure to selectively remove the $|2\rangle$ atoms that fill the nodal plane. The $|2\rangle$ atoms are adiabatically removed over 100 ms, and a bare dark soliton of component $|1\rangle$ remains. The soliton node and any soliton decay products are then too small to be observed while the condensate is held in the trap [18]. We therefore remove the trapping potential and allow the condensate to ballistically expand, causing the variations, or 'defects,' in the condensate density distribution to also expand [19]. These density defects are then resolvable. We obtain a final near-resonance phase-contrast image of the expanded atom cloud, using a probe detuning of 20 MHz. Expansion imaging has previously been used to detect bare vortex cores [4,20].

Numerical calculations – Before discussing experimental data, we briefly describe results of numerical calculations. The techniques employed have been described in detail in Ref. [14]. The equilibrium configuration, dynamics, and Bogoliubov excitation spectrum for a two-component condensate at low temperatures may all be obtained from the appropriate three-dimensional time-dependent Gross-Pitaevskii (GP) equation [21], with $N_1 = 3 \times 10^5$ $|1\rangle$ atoms in a state initially constrained to have odd parity along one axis, and $0 \leq N_2 \leq 7 \times 10^5$ $|2\rangle$ atoms in an even-parity state. The spherical trap frequency is chosen to be $\nu_0 = 7.8$ Hz, and the intra- and inter-species scattering lengths are $(a_{11}\,, a_{22}\,, a_{12}) = 5.5(1.03\,, 0.97\,, 1.0)$ nm, respectively [22]. The behavior of the BEC in full two-component simulations, in which we approximate a slow removal of the $|2\rangle$ atoms, is found to be qualitatively similar to simulations where we set $N_2 = 0$ at the outset. In all cases, the soliton is found to undergo a snake instability, decaying into vortex rings.

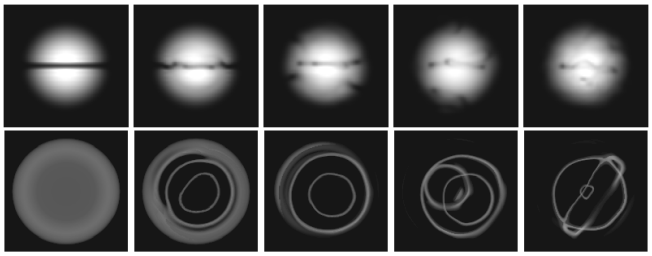

FIG. 1. Results of numerical simulations showing the decay of a black soliton in a BEC. The simulation corresponds to 3×10^5 ^{87}Rb atoms in a spherically symmetric trap with frequency 7.8 Hz. Successive frames are shown at 50 ms intervals, with the first frame at 100 ms after the start of the simulation. The first row shows the density profile of the condensate, integrated down an axis parallel to the soliton plane. The low-density regions within the cloud are also rendered (second row), with views perpendicular to the soliton plane.

Indeed, the Bogoliubov spectrum contains modes with complex frequencies for all N_2 considered; such modes have been shown to drive the soliton instability [14]. For $N_2 \gtrsim 4 \times 10^5$, only one such mode remains, with imaginary frequency of magnitude $\nu \sim (4 \times 10^4/N_2)\nu_0$. Assuming a soliton decay time $\propto \nu^{-1}$, a filled soliton with $N_2 = 7 \times 10^5$ is expected to be stable for longer than 2 s, consistent with experimental observations.

The results of a one-component ($N_2 = 0$) simulation are shown in Fig. 1. The soliton decays into three nearly concentric vortex rings approximately 130 ms after initial formation. In general, the rings tend to migrate towards the condensate surface, and may then grow, shrink, and reconnect with each other. The innermost ring is the most stable, remaining intact for at least 150 ms in the absence of a collision with another ring. Along an imaging axis parallel to the plane of a given vortex ring, the integrated column density reveals two dips in the density distribution, connected by a fainter line. The ring, however, is not constrained to lie in any given plane, and may bend and tilt, producing other types of images. In elongated traps with aspect ratios of two or higher, simulations indicate that a soliton can decay directly into nearly parallel vortex lines rather than rings; however, this behavior is not obtained for spherical traps.

Experimental results – In our experimental cycle, we first create a filled dark soliton and obtain a nondestructive image of the initial trapped (filled) soliton. Over the next 100 ms, we remove the $|2\rangle$ atoms from the soliton nodal plane until only the $|1\rangle$ atoms remain. The trapped single-component condensate is then held for a variable hold time before being allowed to ballistically expand for 56 ms [23]. Finally, the expanded density distribution is recorded.

Images of the decayed solitons typically reveal two dips

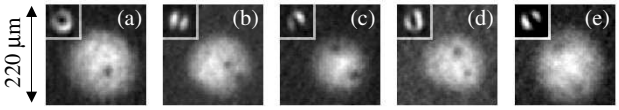

FIG. 2. Typical images of expanded condensates, and their initial states (insets) before the $|2\rangle$ atoms were removed. All images are shown at the indicated scale. (a) A vortex state, (b)-(e) the decay products of solitons. Image (e) was taken with a hold time of 500 ms; all other images were taken with a hold time of 0 ms, in addition to the 100 ms $|2\rangle$ removal and the 56 ms expansion [22].

in the condensate density distribution, as shown in Fig. 2(b)-(e). While our images are consistent with the expected signatures of vortex rings, they are inconclusive evidence for the decay of solitons into vortex rings; from a single image containing only a pair of density dips, we can not differentiate between a *single vortex ring* and a *pair of vortex lines*. For comparison, an expanded vortex line is shown in Fig. 2(a). We believe that our signal-to-noise levels may limit our ability to see a dark line connecting the two clear density defects that would indicate the sides of a ring. We also note that high-frequency excitations visible in $T = 0$ simulations would be quickly damped at finite temperatures, and thus not seen in the experiment.

Because detection of two-dimensional topological structures, such as dark solitons and vortex rings, can be enhanced by probing along two orthogonal directions, we added an additional probe beam. In our improved apparatus, the second probe beam is orthogonal to the original beam, and propagates horizontally (as does the original). The beams intersect at the condensate. Phase-contrast imaging is used independently with each beam path, and the probe beams propagate towards different sides of a single charge-coupled device (CCD) camera array. The apparatus allows us to take simultaneous pictures of condensates from the 'front' (original) and the 'side' (added) directions using a single camera, as illustrated in Fig. 3(a). While we can observe the full depth of the filled soliton node along the front direction, regardless of the initial orientation, the nodal plane is usually at an oblique angle to the side probe, and soliton contrast is thus reduced. Examples of simultaneous images of trapped condensates from the front and side are shown in Figs. 3(b)-(e). In the pair of images shown in Fig. 3(d), the filled core of a vortex is visible as the dark hole in the front image, and as the dark band in the side image. In Fig. 3(e), a filled horizontally oriented dark soliton appears as a band across the condensate in each probing direction, demonstrating that the soliton splits the BEC into two sections.

The use of two orthogonal probe beams confirms that dark solitons indeed decay into vortex rings. With the two beam paths, we have observed pairs of density dips in simultaneous side and front expanded images of decayed

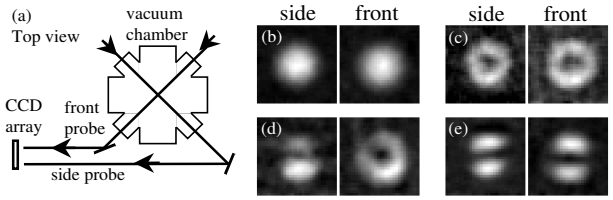

FIG. 3. (a) An illustration of our probe beam imaging paths. (b)-(e) Simultaneous 100-μm-square images of trapped condensates from the front and side imaging directions. Shown are (b) a ground state condensate of component $|1\rangle$, (c) a shell of $|1\rangle$ atoms around a central ball of $|2\rangle$ atoms [21] , (d) a $|1\rangle$ vortex filled with $|2\rangle$ atoms, and (e) a horizontally oriented dark soliton of component $|1\rangle$, filled with $|2\rangle$ atoms.

solitons. In each image set shown in Figs. 4(b)-(d), pairs of density dips lie nearly horizontally and at corresponding locations within the two BEC images. We have also obtained images in which a faint line corresponding to a decrease in integrated column density can be observed between two defects in one of the expanded images, as shown in Figs. 4(e) and (f), providing further striking demonstrations of soliton decay into vortex rings. Figures 4(e)-(g) emphasize that when the vortex ring is not close to horizontal, clear pairs of density dips are not seen in the side images. However, a weak ring-shaped halo may be discerned in the side image residuals of Figs. 4(e) and (g), when the ring is in a near-vertical plane orthogonal to the side probe direction. Although the halo signal is only slightly above the noise of the residuals, it can be noticed when compared to the residuals for an expanded ground state condensate, shown in Fig. 4(a). Images in Figs. 4(b) through (f) represent the best 10% of our data showing solitons decaying into rings; Fig. 4(g) is typical.

Numerical as well as experimental data show great variability in the types of images that can be expected after a soliton decays. For example, Fig. 4(h) is a rare example showing two clear density dips in the side image, but here a clear line corresponding to the defect extends through the entire condensate in the front image and residuals. It is possible that this image shows soliton decay into two vortex lines rather than a ring, or breakup of a ring into vortex lines. We defer to a future paper a discussion of the diversity of our images, which may result from interesting vortex ring dynamics, including vortex ring bending, tilting, and reconnections.

Small perturbations unavoidably induce a dark soliton to decay. In a spherically symmetric BEC, a soliton decays into a relatively stable vortex ring. In addition to demonstrating this nonlinear decay process, our experiment shows that condensates can indeed support vortex rings, which may be detected via expansion imaging. Future experiments may include studies of vortex ring stability, lifetime, and dynamics [24], as well as investigations into vortex structures created by impurity motion above a superfluid critical velocity [25].

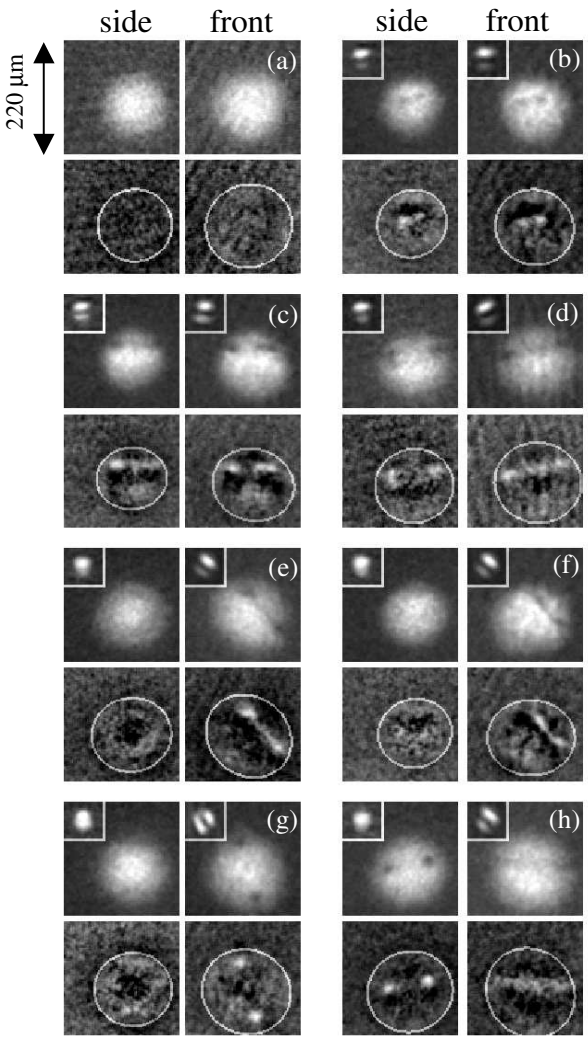

FIG. 4. Images of expanded condensates and their initial states (insets), as viewed along both imaging axes. Each subfigure consists of two expansion images (top row of each subfigure) and two images of residuals plots (bottom row), obtained after subtracting a TF fit of each expansion image. The white regions in the residuals correspond to depletion of fluid in the BEC. The residuals are superimposed with white ellipses outlining the fit TF profiles of the condensates, for position reference. (a) An expanded ground state condensate. (b)-(h) The decay products of solitons. The hold times (between $|2\rangle$-atom removal and BEC expansion) were 0 ms for images (a)-(c),(f), and (g); 50 ms for (d) and (e); and 150 ms for (h).

Possibilities to create vortex rings by other means may also be explored, such as by passing objects through the condensate [26].

We thank Seamus Davis, Murray Holland, and Carl Wieman for helpful discussions. This work was supported by funding from NSF, ONR, and NIST. L.A.C. acknowledges funding from the DOE.

[1] R. Donnelly, *Quantized Vortices in Helium II* (Cambridge University Press, Cambridge, 1991).
[2] D. R. Tilley and J. Tilley, *Superfluidity and Superconductivity, 3rd ed.* (IOP Publishing Ltd, Bristol, 1990).
[3] M. R. Matthews *et al.*, Phys. Rev. Lett. **83**, 2498 (1999).
[4] K. W. Madison, F. Chevy, W. Wohlleben, and J. Dalibard, Phys. Rev. Lett. **84**, 806 (2000).
[5] G. W. Rayfield and F. Reif, Phys. Rev. **136**, A1194 (1964).
[6] See for example, P. G. Drazin and R. S. Johnson, *Solitons: an Introduction* (Cambridge University Press, Cambridge, 1989).
[7] S. Burger *et al*, Phys. Rev. Lett. **83**, 5198 (1999); J. Denschlag *et al*, Science **287**, 97 (2000).
[8] See for example the review article by Y. S. Kivshar and B. Luther-Davies, Phys. Rep. **298**, 82 (1998).
[9] V. Tikhonenko, J. Christou, B. Luther-Davies, and Y. S. Kivshar, Opt. Lett. **21**, 1129 (1996); A. V. Mamaev, M. Saffman, and A. A. Zozulya, Phys. Rev. Lett. **76**, 2262 (1996); A. V. Mamaev, M. Saffman, D. Z. Anderson, and A. A. Zozulya, Phys. Rev. A **54**, 870 (1996).
[10] C. A. Jones, S. J. Putterman, and P. H. Roberts, J. Phys. A **19**, 2991 (1986).
[11] C. Josserand and Y. Pomeau, Europhys. Lett. **30**, 43 (1995).
[12] A. E. Muryshev, H. B. van Linden van den Heuvell, and G. V. Shlyapnikov, Phys. Rev. A **60**, R2665 (1999); P. O. Fedichev, A. E. Muryshev, and G. V. Shlyapnikov, Phys. Rev. A **60**, 3220 (1999).
[13] L. D. Carr, M. Leung, and W. P. Reinhardt, J. Phys. B **33**, 3983 (2000).
[14] D. L. Feder, *et al.*, Phys. Rev. A **62**, 053606 (2000).
[15] W. P. Reinhardt and C. W. Clark, J. Phys. B **30**, L785 (1997).
[16] J. E. Williams and M. J. Holland, Nature **401**, 568 (1999).
[17] Th. Busch and J. R. Anglin, cond-mat/0012354.
[18] The spatial width of a bare dark soliton or vortex core in a pre-expanded sample is on the order of the BEC healing length, about 0.7 μm for our condensates.
[19] F. Dalfovo and M. Modugno, Phys. Rev. A **61**, 023605 (2000).
[20] B. P. Anderson, *et al.*, Phys. Rev. Lett. **85**, 2857 (2000).
[21] H. Pu and N. P. Bigelow, Phys. Rev. Lett **80**, 1134 (1998).
[22] D. S. Hall, *et al.*, Phys. Rev. Lett. **81**, 1539 (1998).
[23] Condensates expand slowly when released from our weak trap. We get larger final spatial distributions by giving the atoms a 6-ms preliminary "squeeze" at high spring constants, followed by a 50-ms expansion period. Dynamical soliton evolution and decay begins during the $|2\rangle$ removal, and continues through about the first few milliseconds of expansion; thereafter, the decay pattern is essentially frozen into the expanding sample.
[24] B. Jackson, C. S. Adams, and J. F. McCann, Phys. Rev. A **61**, 013604 (2000).
[25] R. Onofrio, *et al*, Phys. Rev. Lett. **85**, 2228 (2000).
[26] B. Jackson, C. S. Adams, and J. F. McCann, Phys. Rev. A **60**, 4882 (1999).